PHYSICAL REVIEW B **81**, 020402(R) (2010)

Noncollinear magnetic phases of a triangular-lattice antiferromagnet and of doped $CuFeO_2$

Randy S. Fishman and Satoshi Okamoto
Materials Science and Technology Division, Oak Ridge National Laboratory, Oak Ridge, Tennessee 37831, USA
(Received 8 December 2009; published 6 January 2010)

We obtain the noncollinear ground states of a triangular-lattice antiferromagnet with exchange interactions up to third nearest neighbors as a function of the single-ion anisotropy D. At a critical value of D, the collinear $\uparrow\uparrow\downarrow\downarrow$ phase transforms into a complex noncollinear phase with odd-order harmonics of the fundamental ordering wavevector $\mathbf{Q}$. The observed elastic peaks at $2\pi\mathbf{x}-\mathbf{Q}$ in both Al- and Ga-doped $CuFeO_2$ are explained by a "scalene" distortion of the triangular-lattice produced by the repulsion of neighboring oxygen atoms.

DOI: 10.1103/PhysRevB.81.020402 PACS number(s): 75.30.Ds, 61.05.fg, 75.50.Ee

The noncollinear and multiferroic ground states of frustrated magnetic systems continue to attract intense interest. Due to the strong coupling between the electric polarization and the noncollinear spin states, improper ferroelectric materials hold great technological promise.[1] However, more than one physical mechanism may be responsible for their ferroelectric behavior. An electric polarization $\mathbf{P}$ perpendicular to both the spin rotation axis $\mathbf{S}_i\times\mathbf{S}_j$ and the wave vector $\mathbf{Q}$ is predicted for ferroelectrics with easy-plane anisotropy and spiral spin states such as $R\mathrm{MnO}_3$ ($R=$ Tb or Y).[2] But a simple spiral state is not possible for ferroelectrics based on materials with easy-axis anisotropy such as $CuFeO_2$ (Refs. 3–5) and $MnWO_4$.[6] For Al- or Ga-doped $CuFeO_2$, a modulation of the metal-ligand hybridization with the spin-orbit coupling[7,8] may produce the observed electric polarization $\mathbf{P}$ (Refs. 3–5) parallel to both the spin rotation axis and the wave vector.

In order to clarify the nature of the ferroelectric coupling, it is essential to understand how the noncollinear ground state of an easy-axis ferroelectric evolves with doping. In this paper, we show that the noncollinear ground state of $CuFeO_2$ contains significant odd-order harmonics of the fundamental ordering wave vector $\mathbf{Q}\approx 0.86\pi\mathbf{x}$.[9] The observed elastic peaks at both $\mathbf{Q}$ and $2\pi\mathbf{x}-\mathbf{Q}\approx 1.14\pi\mathbf{x}$ (Refs. 3 and 5) are explained by a distortion of the triangular-lattice associated with the repulsion of neighboring oxygen atoms.

Due to geometric frustration, simple antiferromagnetic (AF) order is not possible on a two-dimensional triangular-lattice with AF interactions $J_1<0$ between neighboring sites. When the easy-axis anisotropy D along the z axis is sufficiently large, however, the anisotropy energy $-D\Sigma_i S_{iz}^2$ favors one of several collinear states. For classical spins, Takagi and Mekata[10] demonstrated that the $\uparrow\uparrow\downarrow\downarrow$ state sketched in Fig. 1 is stable over the range of $J_2/|J_1|$ and $J_3/|J_1|$ plotted in the inset to Fig. 2(a), where J_2 and J_3 are the second- and third-neighbor interactions indicated in Fig. 1 and longer-ranged interactions are neglected. The $\uparrow\uparrow\downarrow\downarrow$ phase with wavevector $\mathbf{Q}_0=\pi\mathbf{x}$ appears in pure $CuFeO_2$ (Refs. 11 and 12) for magnetic fields below about 7 T.

With increasing Al concentration, the spin waves (SWs) of $CuFe_{1-x}Al_xO_2$ soften on either side of $\mathbf{Q}_0$ at wave vectors $\mathbf{Q}_\pm\approx\mathbf{Q}_0\pm 0.14\pi\mathbf{x}$.[13,14] A similar SW softening occurs on a triangular-lattice AF when D is lowered while the exchange constants are fixed.[15] For an Al concentration x greater than $x_c\approx 0.016$ or an anisotropy D lower than $D_c\approx 0.3|J_1|$, the $\uparrow\uparrow\downarrow\downarrow$ phase becomes unstable and a noncollinear phase appears[16,17] with the dominant wavevector $\mathbf{Q}\equiv\mathbf{Q}_-\approx 0.86\pi\mathbf{x}$.

Because the AF interactions between adjacent hexagonal layers of $CuFeO_2$ are not frustrated, the essential physics of $CuFeO_2$ is captured by a two-dimensional triangular-lattice AF with energy

$$E=-\frac{1}{2}\sum_{i\neq j}J_{ij}\mathbf{S}_i\cdot\mathbf{S}_j-D\sum_i S_{iz}^2. \tag{1}$$

A classical approximation for the $S=5/2$ spins of the Fe^{3+} ions incurs only small errors, so each spin $\mathbf{S}_i=\mathbf{S}(\mathbf{R}_i)$ is treated classically with $|\mathbf{S}(\mathbf{R}_i)|=1$. We include exchange couplings J_{ij} up to third nearest neighbors.

Monte Carlo simulations were recently used to study the complex noncollinear (CNC) phase of Eq. (1).[18] Those simulations indicated that the CNC phase interceded between the $\uparrow\uparrow\downarrow\downarrow$ phase at high D and a spiral phase at small D. We have constructed several "trial" spin functions to minimize the energy of Eq. (1), including functions with all three spin components. Those trial functions were motivated by the Fourier peaks in the Monte Carlo solution[18] at wave vectors $\mathbf{Q}=0.87\pi\mathbf{x}$, $1.13\pi\mathbf{x}=2\pi\mathbf{x}-\mathbf{Q}$, and $1.38\pi\mathbf{x}\approx-3\mathbf{Q}+\mathbf{G}$ where $\mathbf{G}=4\pi\mathbf{x}$ is a reciprocal lattice vector.

The trial function with the lowest energy contains odd-order harmonics in an expansion of the spin:

$$S_z(\mathbf{R})=A\Big\{\cos(Qx)+\sum_{l=1}C_{2l+1}\cos[Q(2l+1)x]+\sum_{l=0}B_{2l+1}\cos[Q'(2l+1)x+\phi]\Big\}, \tag{2}$$

$$S_y(\mathbf{R})=\sqrt{1-S_z(\mathbf{R})^2}\,\mathrm{sgn}[\sin(Qx)], \tag{3}$$

where $\mathbf{Q}'=2\pi\mathbf{x}-\mathbf{Q}$. Notice that $\mathbf{S}(\mathbf{R})=\mathbf{S}(x)$ depends only on x. The anharmonic coefficients $C_{2l+1>1}$ reflect the deviation from a pure cycloid with $\mathbf{S}(x)=[0,\sin(Qx),\cos(Qx)]$; the coefficients B_{2l+1} are produced by a lattice distortion with period 1, as discussed further below. The amplitude A is fixed by the constraint that $\max|S_z(x)|=1$ and the lattice constant is set to 1. Keep in mind that $\mathbf{Q}$ and $\mathbf{Q}'$ are distinct wave vectors not related by a reciprocal lattice vector.

Like the observed multiferroic phase,[3] the CNC phase of Eqs. (2) and (3) is coplanar with the spin rotation axis $\mathbf{S}(x)$

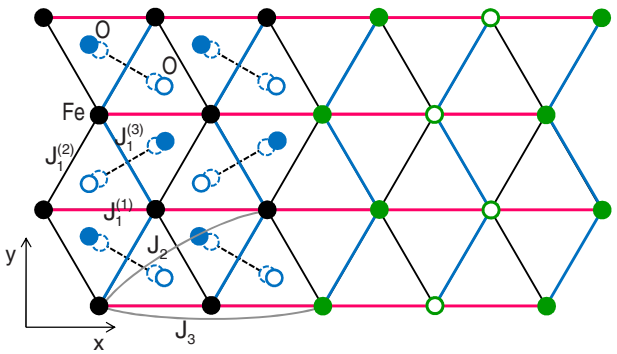

FIG. 1. (Color online) The exchange constants $J_1^{(i)}$, J_2, and J_3, and the oxygen displacements responsible for the scalene distortion of the lattice. The thick bonds $J_1^{(3)}=J_1+K_1$ form a zigzag pattern. Also shown is the $\uparrow\uparrow\downarrow\downarrow$ state with $\uparrow$ (solid) and $\downarrow$ (open) spins. For $K_1>0$, $J_1^{(3)}$ couples the same spin along each zigzag.

$\times\mathbf{S}(x+1/2)$ parallel to $\mathbf{Q}$ along the x axis. A uniform rotation of $\mathbf{S}(x)$ about the z axis would not cost any anisotropy energy but would cost magnetoelastic energy due to the distortions discussed below.

As shown in Ref. 18, the dominant wave vector of the CNC phase coincides with the wave vector of the dominant SW instability of the $\uparrow\uparrow\downarrow\downarrow$ phase. Depending on whether the exchange parameters $\{J_2/|J_1|, J_3/|J_1|\}$ fall within regions 4I or 4II plotted in the inset to Fig. 2(a), the dominant SW instability occurs either at a variable wavevector $\mathbf{Q}$ (region 4I) or at $(4\pi/3)\mathbf{x}$ (region 4II).[19] The exchange parameters used in Fig. 2(a) ($J_2/|J_1|=-0.20$, $J_3/|J_1|=-0.26$) fall within region 4II; the exchange parameters used in Fig. 2(b) ($J_2/|J_1|=-0.44$, $J_3/|J_1|=-0.57$) fall within region 4I. The latter are believed to correspond approximately to the ratio of exchange parameters in pure $CuFeO_2$.[14] With those parameters, the dominant SW instability of the $\uparrow\uparrow\downarrow\downarrow$ phase and the dominant ordering wave vector of the CNC phase are both $\mathbf{Q}\approx\mathbf{Q}_0-0.14\pi\mathbf{x}=0.86\pi\mathbf{x}$. The wave vector of the third harmonic $3\mathbf{Q}$ is then equivalent to $1.42\pi\mathbf{x}$.[9]

The classical energy E was minimized within a unit cell of length 5,000 with open boundary conditions in the x direction. Doubling the unit cell has no noticeable effect on the amplitudes plotted in Figs. 2(a) and 2(b). In the absence of a lattice distortion, the amplitudes B_{2l+1} are negligible but the higher harmonics $C_{2l+1>1}$ are significant. For all $D/|J_1|$, the trial spin configuration has a lower energy than the Monte Carlo state. Notice that the anharmonicity in region 4II is much weaker than in region 4I. For the parameters of Fig. 2(a), only the third and fifth harmonics C_3 and C_5 are significant; for the parameters of Fig. 2(b), harmonics above C_7 can be neglected. The S_z component of the anharmonic CNC phase within region 4I is sketched in the inset to Fig. 2(b). This phase retains some of the Ising character of the $\uparrow\uparrow\downarrow\downarrow$ phase with $\langle S_z^2\rangle=0.72$ at $D/|J_1|=0.3$.

Within region 4II, $\mathbf{Q}=4\pi\mathbf{x}/3$ depends on neither the exchange parameters nor the anisotropy; within region 4I, $\mathbf{Q}$ is relatively insensitive to D but sensitively depends on the ratio of exchange parameters, as discussed in Refs. 18 and 19. For the parameters used in Fig. 2(b), $\mathbf{Q}\approx 0.857\pi\mathbf{x}$.

With decreasing D, the anharmonicity decreases in both regions 4I and 4II. Pure spirals with $C_{2l+1>1}=0$ and $\langle S_z^2\rangle=0.5$ are recovered as $D\to 0$. So the phase diagram provided by Fig. 3 of Ref. 18 should be revised to eliminate the sharp boundary between the CNC phase and the spiral region. Comparing the numerical results obtained for the trial spin configuration of Eqs. (2) and (3) with the earlier Monte Carlo results[18] using the parameters of Fig. 2(b), we find that the critical value D_c below which the $\uparrow\uparrow\downarrow\downarrow$ phase becomes unstable increases from $0.295|J_1|$ to $0.317|J_1|$. When $D/|J_1|=0.1$, the energy of the Monte Carlo phase is $E/N=-1.284|J_1|$ whereas the energy of the anharmonic CNC phase is $-1.295|J_1|$. These energies can be compared with the energy of the $\uparrow\uparrow\downarrow\downarrow$ phase in Fig. 3(b).

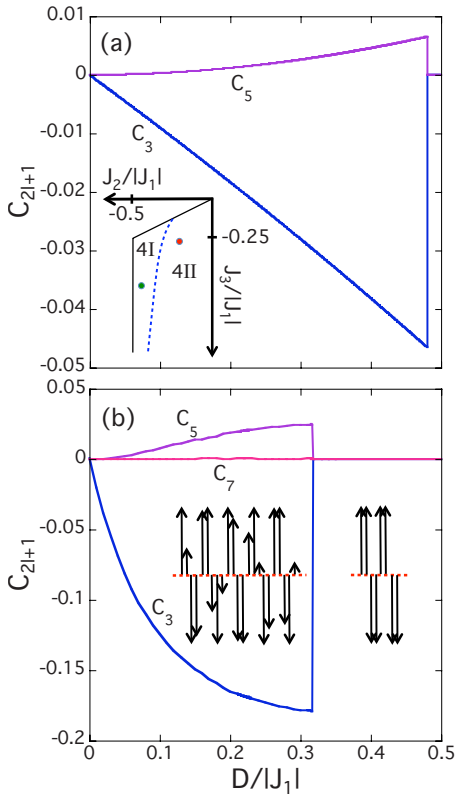

FIG. 2. (Color online) The harmonic amplitudes C_{2l+1} as a function of $D/|J_1|$ for (a) $J_2/|J_1|=-0.20$ and $J_3/|J_1|=-0.26$ or (b) $J_2/|J_1|=-0.44$ and $J_3/|J_1|=-0.57$. Inset in (a) is the phase diagram indicating regions 4I and 4II discussed in the text with the red dot (region 4II) corresponding to the (a) parameters and the blue dot (region 4I) to the (b) parameters. In (b) we sketch the $\uparrow\uparrow\downarrow\downarrow$ phase stable above $D/|J_1|=0.32$ and the CNC phase (S_z component only) at $D/|J_1|=0.3$.

The observed $2\pi\mathbf{x}-\mathbf{Q}$ peak in the elastic neutron-scattering measurements[3,5] with amplitude $|B_1|^2$ is absent for a nondistorted lattice. This elastic peak requires a lattice distortion with a wave vector of $\mathbf{q}=2\pi\mathbf{x}$ or a period of 1. The most likely source of that distortion is the repulsion of neighboring oxygen atoms shown in Fig. 1. For each pair of oxygen atoms, one lies below the hexagonal layer and the other lies above. The displacement of oxygen atoms pictured in Fig. 1 produces a "scalene" distortion of the triangular-lattice that has been observed in both the low-field $\uparrow\uparrow\downarrow\downarrow$ phase of pure $CuFeO_2$ as well as in the field-induced multiferroic

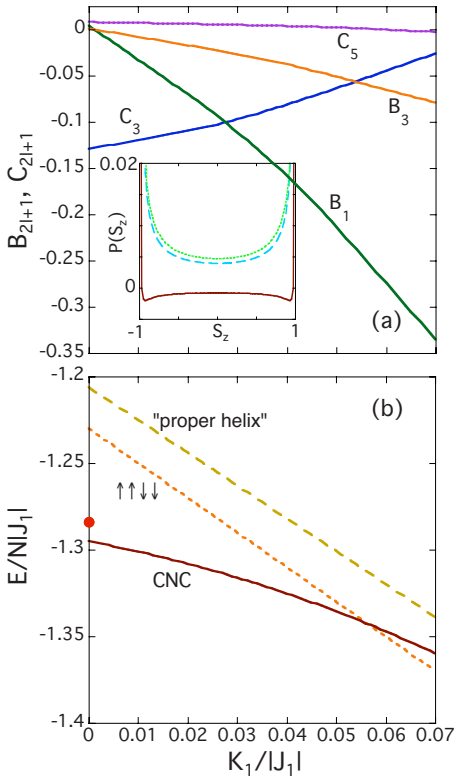

FIG. 3. (Color online) (a) The amplitudes B_{2l+1} and C_{2l+1} versus the distortion K_1 for $D/|J_1|=0.1$. Inset are the spin populations $P(S_z)$ for the spin states at $K_1=0$ (long dash) and $K_1/|J_1|=0.05$ (short dash) as well as their difference (solid). (b) The energy $E/N|J_1|$ for the predicted CNC phase (solid), the $\uparrow\uparrow\downarrow\downarrow$ phase (short dash) and the "proper helix" (Ref. 3) (long dash). The dot along the E axis is the energy of the Monte Carlo simulation. (Ref. 18) Other parameters as in Fig. 2(b).

phase above 7 T.[20] It has also been reported in the ferroelectric phase of Al-doped $CuFeO_2$.[4] The displacement expands the lattice in the x direction,[21] as observed in pure $CuFeO_2$.[20,22]

To study the distorted phase, we take $J_1^{(1)}=J_1^{(2)}=J_1-K_1/2$ and $J_1^{(3)}=J_1+K_1$, which ensures that the average bond strength remains J_1. The energy K_1 measures the degree of distortion of the nearest-neighbor exchange. When $K_1>0$, the oxygen displacements weaken the AF coupling $J_1^{(3)}$ and strengthen the AF couplings $J_1^{(1)}$ and $J_1^{(2)}$. The $J_1^{(3)}$ bonds form a zigzag pattern with wave vector $2\pi\mathbf{x}$ or a period of 1. The lattice distortion lowers the energy of the $\uparrow\uparrow\downarrow\downarrow$ phase, which is given by $E/N=J_1-J_2+J_3-D-2K_1$ for $K_1>0$ and $E/N=J_1-J_2+J_3-D+K_1$ for $K_1<0$. For $K_1>0$, the $\uparrow$ or $\downarrow$ spins prefer to lie on the same zigzag coupled by the weakest AF bond $J_1^{(3)}$, as shown in Fig. 1. By breaking the threefold degeneracy of the energy, this distortion selects a spin state with wave vector along $\mathbf{x}$ over its two twins with wave vectors rotated by $\pm\pi/3$.

The amplitudes B_{2l+1} and C_{2l+1} are plotted versus $K_1/|J_1|$ for $D/|J_1|=0.1$ in Fig. 3(a). The phase ϕ in Eq. (2) is fixed by the phase of the lattice distortion. With increasing $K_1/|J_1|$, the third-order amplitude C_3 decreases while the amplitudes B_1 and B_3 increase in size. For $K_1/|J_1|=0.05$, $B_1\approx-0.21$ and $B_3\approx-0.05$. The anharmonicity of the spin changes with the distortion: $\langle S_z^2\rangle$ decreases from 0.65 to 0.59 as K_1 increases from 0 to $0.05|J_1|$. Spin population profiles $P(S_z)$ for $K_1=0$ and $K_1=0.05|J_1|$ are plotted in the inset to Fig. 3(a). Their difference indicates that the distorted lattice is more heavily weighted toward $S_z=0$ and the nondistorted lattice is more heavily weighted toward $S_z=\pm1$. As shown in Fig. 3(b), the $\uparrow\uparrow\downarrow\downarrow$ phase obtains a lower energy than the CNC phase when $K_1>0.057|J_1|$.

Other distortions of the lattice with a period of 1 along $\mathbf{x}$ can also produce sizeable amplitudes B_1 at the wave vector $2\pi\mathbf{x}-\mathbf{Q}$. However, the $2\pi\mathbf{x}-\mathbf{Q}$ peak cannot be induced by the $\mathbf{q}=0$ "isosceles" distortion observed by Feng *et al.*[22] in pure $CuFeO_2$ with the $J_1^{(1)}$ bonds along the x axis reduced in size but the diagonal bonds $J_1^{(2)}=J_1^{(3)}$ remaining identical.

Guided by the observed elastic peaks at $\mathbf{Q}$ and $2\pi\mathbf{x}-\mathbf{Q}$, Nakajima *et al.*[3] constructed a CNC phase different than the one proposed here. Their "proper helix" is a modified spiral with the same spin on sites $\mathbf{R}=m\mathbf{x}+n\sqrt{3}\mathbf{y}$ and $\mathbf{R}'=\mathbf{R}+\mathbf{x}/2+\sqrt{3}\mathbf{y}/2$. After minimizing its energy as a function of wave vector for $D/|J_1|=0.1$, we compare the proper helix with the predicted CNC phase as well as with the pure $\uparrow\uparrow\downarrow\downarrow$ phase in Fig. 3(b). Not only does the proper helix have a higher energy than the predicted CNC phase, it also has a higher energy than the $\uparrow\uparrow\downarrow\downarrow$ phase provided that $D/|J_1|$ is not too small. For a nondistorted lattice with $K_1=0$, the proper helix has a lower energy than the $\uparrow\uparrow\downarrow\downarrow$ phase (but not lower than the predicted CNC phase) when $D/|J_1|<0.047$.

Estimating the actual distortion in $CuFeO_2$ requires that we also consider the elastic energy cost proportional to K_1^2. Since the gain in exchange energy in Fig. 3(b) is linear in K_1, a distortion with period 1 occurs in both the $\uparrow\uparrow\downarrow\downarrow$ and the CNC phases. Allowing a general distortion of the lattice with wave vector $\mathbf{q}$, we find that the energy also has minima at $\mathbf{q}=2\mathbf{Q}$ and $4\pi\mathbf{x}-2\mathbf{Q}$, corresponding to a charge modulation with half the period of the spin modulation. This modulation has been observed[4] in Al-doped $CuFeO_2$ and may be related to the predicted ferroelectric instability,[8] which contains both second- and fourth-order harmonics in addition to the uniform displacement of the oxygen atoms.

Of course, it remains possible that the trial spin state used in this work is incomplete and that an even lower-energy state can be achieved. But the close agreement with Monte Carlo simulations[18] in Fig. 3(b) bolsters our confidence that the anharmonic CNC state provides an excellent approximation to the true ground state of Eq. (1) for classical spins. As a test of our model, Fig. 3(a) indicates that the multiferroic state should have small elastic peaks at the third harmonics of $\mathbf{Q}$ and $\mathbf{Q}'$.[9]

To summarize, we have shown that the CNC phase of a frustrated triangular-lattice contains significant odd-order harmonics of the fundamental wave vector $\mathbf{Q}$. This result should greatly facilitate the future modeling of multiferroic ground states. As the easy-axis anisotropy D is reduced, the amplitudes of the higher harmonics are decreased and a pure cycloid is recovered as $D\to0$. The $2\pi\mathbf{x}-\mathbf{Q}$ peaks observed in Al- and Ga-doped $CuFeO_2$ are explained by the scalene distortion of the triangular-lattice.

This research was sponsored by the Division of Materials Sciences and Engineering of the U.S. Department of Energy.

[1] D. I. Khomskii, J. Magn. Magn. Mater. **306**, 1 (2006); S.-W. Cheong and M. Mostovoy, Nature Mater. **6**, 13 (2007).

[2] H. Katsura, N. Nagaosa, and A. V. Balatsky, Phys. Rev. Lett. **95**, 057205 (2005); M. Mostovoy, *ibid.* **96**, 067601 (2006).

[3] T. Nakajima, S. Mitsuda, S. Kanetsuki, K. Prokes, A. Podlesnyak, H. Kimura, and Y. Noda, J. Phys. Soc. Jpn. **76**, 043709 (2007); T. Nakajima, S. Mitsuda, S. Kanetsuki, K. Tanaka, K. Fujii, N. Terada, M. Soda, M. Matsuura, and K. Hirota, Phys. Rev. B **77**, 052401 (2008).

[4] T. Nakajima, S. Mitsuda, T. Inami, N. Terada, H. Ohsumi, K. Prokes, and A. Podlesnyak, Phys. Rev. B **78**, 024106 (2008).

[5] N. Terada, T. Nakajima, S. Mitsuda, H. Kitazawa, K. Kaneko, and N. Metoki, Phys. Rev. B **78**, 014101 (2008).

[6] A. H. Arkenbout, T. T. M. Palstra, T. Siegrist, and T. Kimura, Phys. Rev. B **74**, 184431 (2006); K. Taniguchi, N. Abe, T. Takenobu, Y. Iwasa, and T. Arima, Phys. Rev. Lett. **97**, 097203 (2006).

[7] C. Jia, S. Onoda, N. Nagaosa, and J. H. Han, Phys. Rev. B **74**, 224444 (2006).

[8] T. Arima, J. Phys. Soc. Jpn. **76**, 073702 (2007).

[9] In a three-dimensional crystal, the instability and ordering wave vectors all have a z component of 3/2 in units of $2\pi/c$, where the separation between layers is $c/3$. In (H,K,L) notation, $\mathbf{Q} \approx (0.21, 0.21, 3/2)$, $\mathbf{Q}' = 2\pi\mathbf{x} - \mathbf{Q} \approx (0.29, 0.29, 3/2)$, the third harmonic of $\mathbf{Q}$ is equivalent to (0.37, 0.37, 3/2), and the third harmonic of $\mathbf{Q}'$ is equivalent to (0.13, 0.13, 3/2).

[10] T. Takagi and M. Mekata, J. Phys. Soc. Jpn. **64**, 4609 (1995).

[11] S. Mitsuda, H. Yoshizawa, N. Yaguchi, and M. Mekata, J. Phys. Soc. Jpn. **60**, 1885 (1991).

[12] M. Mekata, N. Yaguchi, T. Takagi, T. Sugino, S. Mitsuda, H. Yoshizawa, N. Hosoito, and T. Shinjo, J. Phys. Soc. Jpn. **62**, 4474 (1993).

[13] N. Terada, S. Mitsuda, Y. Oohara, H. Yoshizawa, and H. Takei, J. Magn. Magn. Mater. **272-276**, e997 (2004); N. Terada, S. Mitsuda, K. Prokes, O. Suzuki, H. Kitazawa, and H. A. Katori, Phys. Rev. B **70**, 174412 (2004); N. Terada, S. Mitsuda, T. Fujii, and D. Petitgrand, J. Phys. Condens. Matter **19**, 145241 (2007).

[14] F. Ye, J. A. Fernandez-Baca, R. S. Fishman, Y. Ren, H. J. Kang, Y. Qiu, and T. Kimura, Phys. Rev. Lett. **99**, 157201 (2007); R. S. Fishman, F. Ye, J. A. Fernandez-Baca, J. T. Haraldsen, and T. Kimura, Phys. Rev. B **78**, 140407(R) (2008).

[15] R. S. Fishman, J. Appl. Phys. **103**, 07B109 (2008).

[16] S. Kanetsuki, S. Mitsuda, T. Nakajima, D. Anazawa, H. A. Katori, and K. Prokes, J. Phys. Condens. Matter **19**, 145244 (2007).

[17] S. Seki, Y. Yamasaki, Y. Shiomi, S. Iguchi, Y. Onose, and Y. Tokura, Phys. Rev. B **75**, 100403(R) (2007).

[18] J. T. Haraldsen, M. Swanson, G. Alvarez, and R. S. Fishman, Phys. Rev. Lett. **102**, 237204 (2009).

[19] M. Swanson, J. T. Haraldsen, and R. S. Fishman, Phys. Rev. B **79**, 184413 (2009).

[20] N. Terada, S. Mitsuda, H. Ohsumi, and K. Tajima, J. Phys. Soc. Jpn. **75**, 023602 (2006); N. Terada, Y. Tanaka, Y. Tabata, K. Katsumata, A. Kikkawa, and S. Mitsuda, *ibid.* **75**, 113702 (2006).

[21] An expansion of the lattice in the x direction will also suppress the magnitude of $J_1^{(1)}$ compared to $J_1^{(2)}$. However, a uniform change in $J_1^{(1)}$ (with wave vector $\mathbf{q}=0$) does not produce any additional elastic peaks.

[22] F. Ye, Y. Ren, Q. Huang, J. A. Fernandez-Baca, P. Dai, J. W. Lynn, and T. Kimura, Phys. Rev. B **73**, 220404(R) (2006).